



Natural Resources
Canada

Ressources naturelles
Canada

**GEOLOGICAL SURVEY OF CANADA
OPEN FILE 9225**

**Canadian ThermoCHronology (CATCH) database:
northern Canada compilation**

J.W. Powell, D.A. Kellett, F. Kohlmann, and M. McMillan

2025

Canada 

**GEOLOGICAL SURVEY OF CANADA
OPEN FILE 9225**

**Canadian ThermoCHronology (CATCH) database:
northern Canada compilation**

J.W. Powell¹, D.A. Kellett², F. Kohlmann³, and M. McMillan^{3,4}

¹Natural Resources Canada, Geological Survey of Canada, 601 Booth Street, Ottawa, Ontario K1A 0E8

²Natural Resources Canada, Geological Survey of Canada, 1 Challenger Drive, P.O. Box 1006, Dartmouth, Nova Scotia B2Y 4A2

³Lithodat Pty Ltd, 94 Stephensons Road, Melbourne 3149, Australia

⁴The University of Melbourne, Grattan Street, Parkville, Victoria 3010, Australia

2025

© His Majesty the King in Right of Canada, as represented by the Minister of Natural Resources, 2025

Information contained in this publication or product may be reproduced, in part or in whole, and by any means, for personal or public non-commercial purposes, without charge or further permission, unless otherwise specified.

You are asked to:

- exercise due diligence in ensuring the accuracy of the materials reproduced;
- indicate the complete title of the materials reproduced, and the name of the author organization; and
- indicate that the reproduction is a copy of an official work that is published by Natural Resources Canada (NRCan) and that the reproduction has not been produced in affiliation with, or with the endorsement of, NRCan.

Commercial reproduction and distribution is prohibited except with written permission from NRCan. For more information, contact NRCan at copyright-droitdauteur@nrcan-rncan.gc.ca.

This publication is available for free download through the NRCan Open Science and Technology Repository (<https://ostrnrcan-dostrnrcan.canada.ca/>).

Recommended citation

Powell, J.W., Kellett, D.A., Kohlmann, F., and McMillan, M., 2025. Canadian ThermoCHronology (CATCH) database: northern Canada compilation; Geological Survey of Canada, Open File 9225, 1 .zip file.
<https://doi.org/10.4095/pdreqf905k>

Publications in this series have not been edited; they are released as submitted by the author.

ISSN 2816-7155
ISBN 978-0-660-74235-9
Catalogue No. M183-2/9225E-PDF
<https://doi.org/10.4095/pdreqf905k>

Introduction

Low-temperature thermochronometers, such as the fission track and (U-Th)/He systems, are radiometric dating methods that are sensitive to low (<~300°C) temperature regimes that are characteristic of relatively shallow depths in the Earth's crust (Fig. 1). As a result, low-temperature thermochronology (LTT) provides temporal constraints on a range of important upper crustal geological processes, such as tectonic and climatic exhumation, brittle deformation, sedimentary burial, hydrothermal fluid circulation and changes in crustal heat flow over time. The unique ability of LTT to unravel the thermal history of rocks renders these methods invaluable for assessing the geodynamic and surficial processes that have impacted Canada's bedrock throughout geologic time.

Over the last several decades, LTT methods have become increasingly popular due to continued advancements in our understanding of the physicochemical processes within mineral crystal lattices that control isotopic diffusion and damage annealing at low temperatures (Fig. 2). For example, the fission track dating method, in which damage zones, or tracks, within crystal lattices are formed due to the spontaneous fission of ^{238}U atoms, was originally pioneered in the 1960s (Price and Walker 1963; Naeser 1967; Wagner 1968), and saw increased application from the 1980s onwards following the discovery and characterization of some of the fundamental thermal, chemical and crystallographic controls on fission track annealing in apatite (e.g. Gleadow & Duddy, 1981; Green, 1980). In comparison, the (U-Th)/He method, in which ^4He is the radiogenic daughter product of U, Th, and Sm, was the first geochronometer applied to date zircon (Strutt 1909, 1910). These original studies determined that the calculated ages were too young to be crystallization ages due to 'leaky helium'. The (U-Th)/He method only saw renewed interest following studies that identified thermal controls on helium diffusion (Zeitler *et al.* 1987), the effects of radiogenic helium ejection on (U-Th)/He age (Farley *et al.* 1996) and laboratory-defined helium diffusion kinetics (e.g. Flowers 2009; Gautheron *et al.* 2009; Guenther *et al.* 2013). Now, there are numerous LTT laboratories across the globe, including several in Canada, that generate thousands of analyses and hundreds of publications each year.

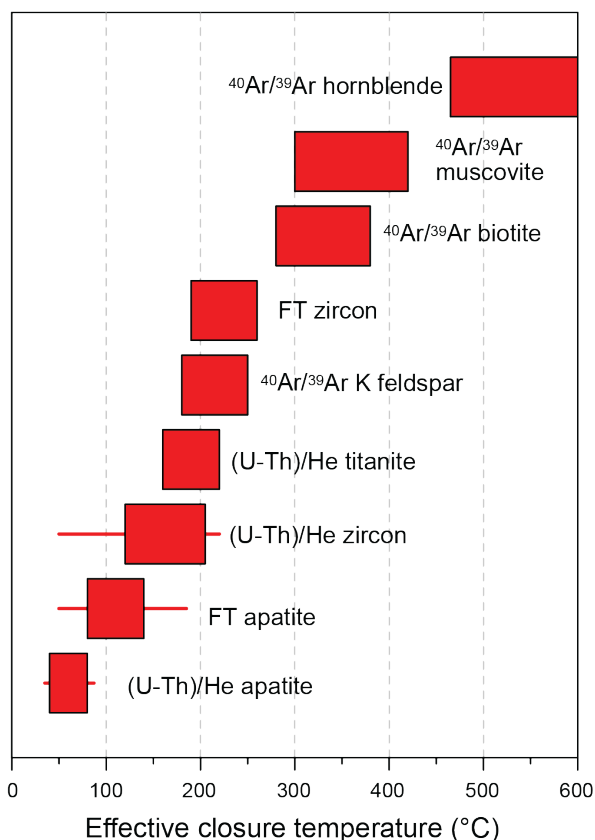


Figure 1. Closure temperatures of various thermochronometers for cooling rates from 0.1 – 100°C/m.y (red bars; modified after Reiners & Brandon 2006). Red lines indicate expanded temperature sensitivity on the basis of radiation damage (Flower *et al.* 2009; Guenther *et al.* 2013) and mineral composition (Djimbi *et al.* 2015; Issler *et al.* 2022). Fission track and (U-Th)/He thermochronology data are captured in this compilation.

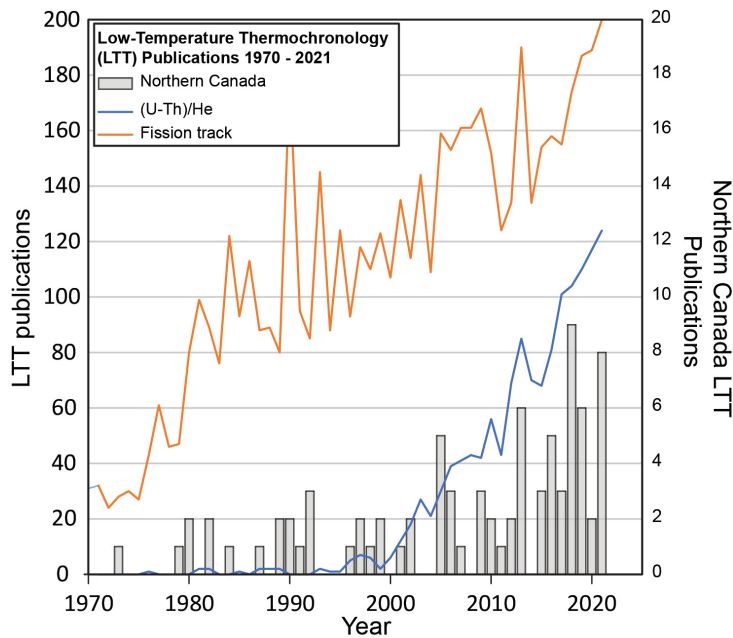


Figure 2. Charting the number of LTT publications from 1970 - 2021. The number of (U-Th)/He and fission track publications per year were extracted from Scopus.com whereas the northern Canada publications are collated in this report

In comparison with other geochronometers, such as those employing the U-Pb and K-Ar decay systems, which tend to provide robust crystallization and cooling ages, LTT methods commonly exhibit significant intrasample date dispersion related to geologic history, elevation, cooling rate, grain size and mineral composition (e.g. Carlson *et al.* 1999; Ketcham *et al.* 1999; Armstrong 2005; Reiners and Brandon 2006; Shuster *et al.* 2006). As a result, measured LTT dates are not always reflective of a cooling age and data are frequently interpreted via numerical modelling methods (Issler 1996; Ketcham 2005, 2024; Gallagher 2012, 2023) that use laboratory-defined kinetic models of thermal diffusion and annealing to understand the time-temperature implications of measured LTT data and corresponding kinetic parameters. As a result, LTT methods have unique requirements for data reporting relative to other geochronometers (Flowers *et al.* 2023a, b; Kohn *et al.* 2024), as both the analytical methods for deriving LTT dates and various metadata are important for thermal history modelling and must be captured.

Given the fact that kinetic models for annealing and diffusion are routinely updated and improved upon, and new software and codes for numerical modelling thermal histories are routinely published, the ability to re-interrogate published data through a modern lens is important to present-day and future low-temperature thermochronologists. This is an especially important consideration given the ongoing push to develop big data approaches to deriving regional geologic histories from large LTT datasets (Fox *et al.* 2014, 2016; Boone *et al.* 2023; van der Beek and Schildgen 2023). In order for LTT data to be functionally reuseable, the data need to be compiled in a purpose-built structure that accounts for the different thermochronometers, the various generations of data and the corresponding metadata. This can be extremely laborious due to the variety and volume of the required data attributes: for example, a single apatite fission track age from an older publication might only include an age and error, whereas a modern sample could have >3000 unique entries (Boone *et al.* 2023). Given the rapid increase in LTT publications (Fig. 2), unique data structures tailored to LTT are required to accommodate the volume of new analyses and associated metadata.

Although the Geological Survey of Canada's (GSC) geochronology laboratories do not produce LTT data, the GSC has facilitated production of many of the existing Canadian LTT datasets through internal research projects, external grants and access to the extensive GSC sample archives. Presently,

only apatite fission track dates are captured in a preliminary compilation (Pinet & Brake, 2018), and neither fission track nor (U-Th)/He data and metadata are collated in any database. The absence of a central database is of growing concern, given the surging popularity of these methods and their wide applicability to Canadian geoscience studies. This publication addresses this concern by providing a comprehensive compilation of all northern Canada fission track and (U-Th)/He data published from 1970-2021 (Figs. 2, 3) and marks the first step towards the GSC's new CANadian ThermoCHronology (CATCH) database. The goal of the CATCH database is to provide the geoscience community with a *FAIR* (Findable, Accessible, Interoperable, Reuseable) tool for accessing Canadian LTT data. This publication is the first in a series of three Open Files, with the subsequent open files detailing: 1) an LTT compilation for southern Canada, as well as a compilation of all LTT thermal history models and metadata; 2) an open file detailing the CATCH database and templates for how thermochronologists can

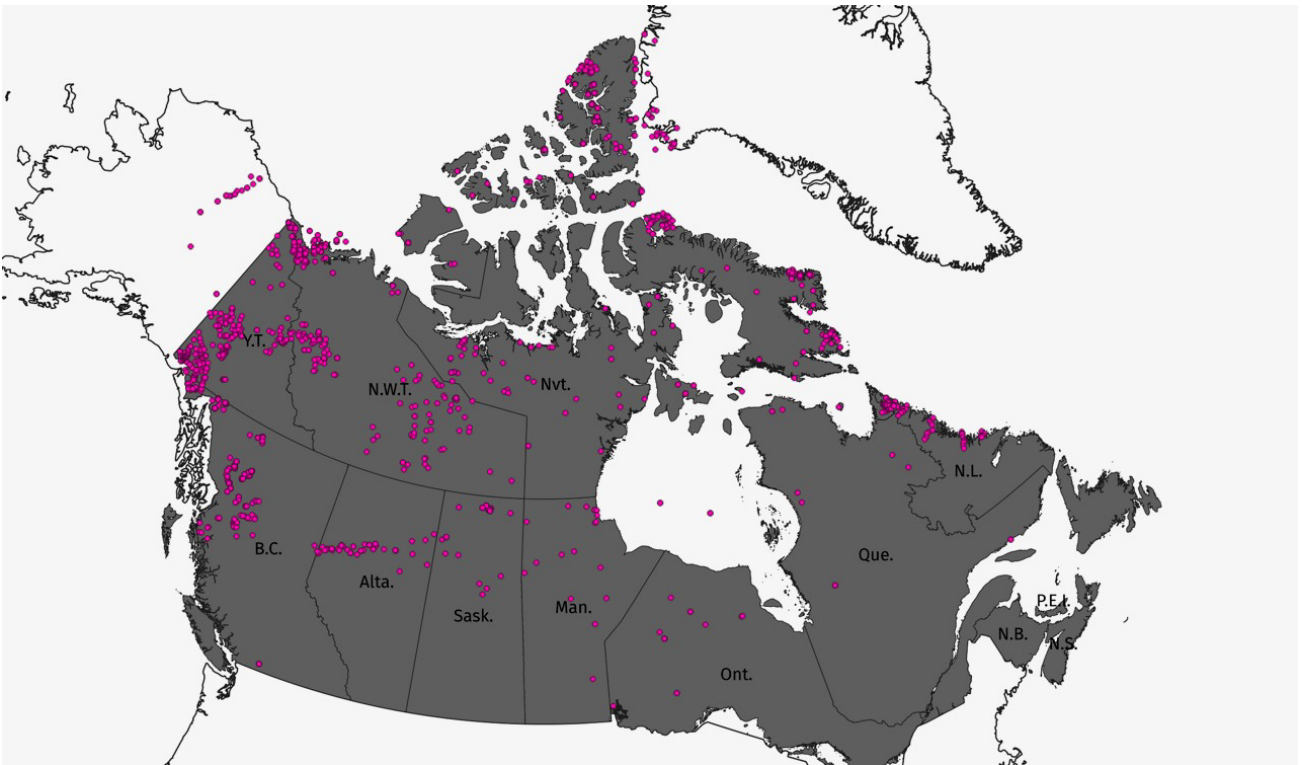


Figure 3. Locations of samples with LTT data in northern Canada. All published data are included in this report. Note: data from Alaska, Greenland and southern Canada were also extracted if included in the same publications as northern Canada LTT data.

submit their published data for curation. Data from the CATCH compilations will also be publicly accessible via the open-access *AusGeochem* data platform (<https://ausgeochem.auscope.org.au>).

LTT Data Extraction and Curation

Data extraction involved extensive data mining of all LTT data and associated metadata for northern Canada. Data extraction from modern publications was straightforward as most tables are digital and could be copied and pasted into a structured format such as Microsoft Excel. In the case of analogue paper reports or older pdfs without vectorized metadata, data were extracted manually or using additional data extraction steps. Every extracted row of data underwent quality control to ensure no errors occurred in conversion. At the sample level, we capture sample metadata (name, coordinates, location name and description, location type, sampling method, rock type, stratigraphic unit and elevation). For publications where sample coordinates were not provided, the locations were determined

via georeferencing (Fig. 4). This compilation also captures any international LTT data that were included in publications with Canadian LTT data. In addition to the sample, fission track and (U-Th)/He data, we also record important metadata corresponding to funding sources, chief investigator, analysts, laboratory and literature reference for all samples. The full data compilation is included in the supplementary data for this publication.

The data fields for the fission track compilation were designed to match modern data reporting requirements (Kohn *et al.* 2024). A lengthy description of each field is outside the scope of this open file, but a glossary of terms is provided in Table 1 and readers can refer to Kohn *et al.* (2024) for a detailed description of pertinent data fields in fission track thermochronology. In general, the ‘FT Datapoints’ tab summarizes bulk fission track (FT) data for all samples, whereas ‘FT Count Data’ and ‘FT Single Grain’ tabs capture the fission track counting statistics and corresponding age and uranium concentration for the samples for which single grain fission track data are available. A sample may have multiple entries in ‘FT Data Points’ if it was analyzed multiple times or reinterpreted in a subsequent publication. Individual fission track lengths, when reported, are captured in the ‘FT Length Data’. When comprehensive length data are not available in publications, fission track lengths are digitized from length distribution histograms and the binned length values are reported in the ‘FT Binned Length Data’ (Fig. 5).

In a similar fashion to the fission track compilation, the (U-Th)/He compilation follows the thermochronology community’s guidelines for data reporting (Flowers *et al.* 2023a, b). Table 2 provides a glossary of pertinent terms for our data compilation, and readers can refer to the work of Flowers *et al.* (2023a, b) for a detailed description of the (U-Th)/He method and pertinent data fields. In our compilation, the ‘He Datapoints’ tab includes all samples with (U-Th)/He data and references the mean (U-Th)/He date, if reported. The ‘He Whole Grain’ tab includes detailed information on the analyses for multi-grain or single grain aliquots.

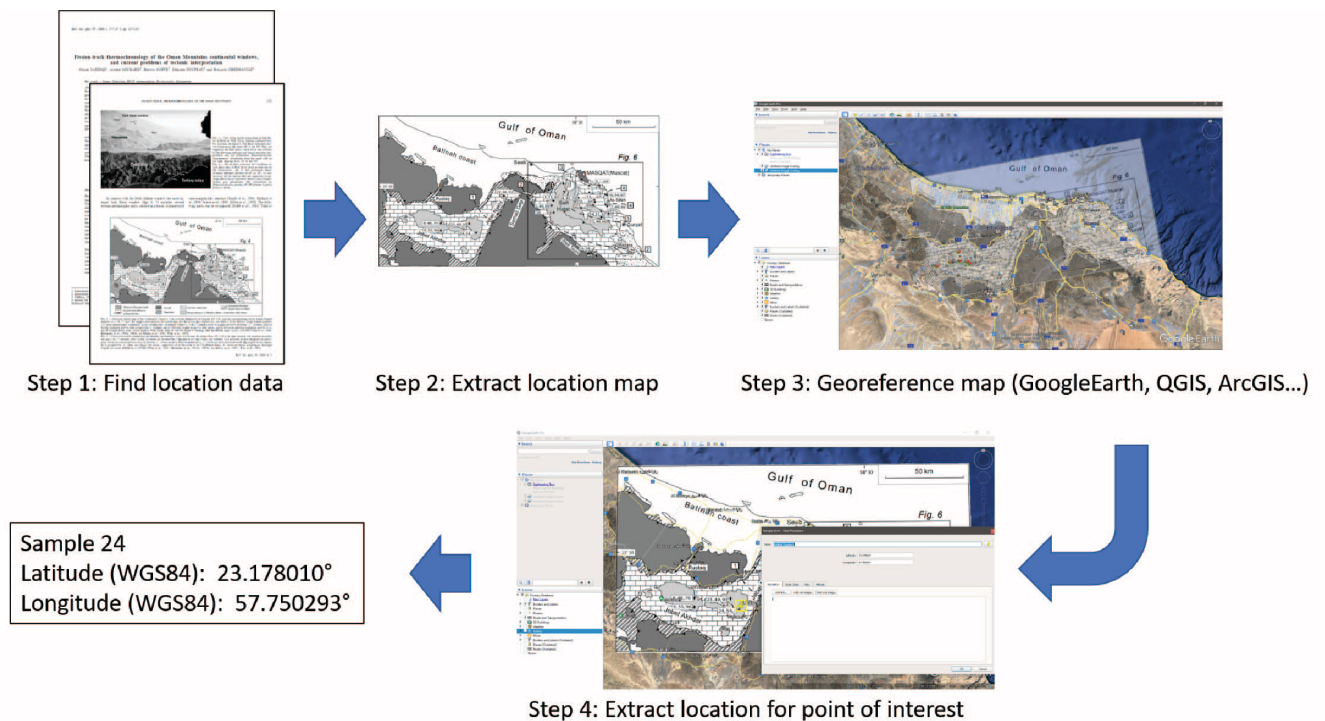


Figure 4. (previous page) Sample coordinates are not provided in many publications. To capture the most accurate location possible, we extracted the geologic maps and georeferenced the samples. In addition to location, the database captures other pertinent geologic metadata fields (lithology, stratigraphic unit, age, tectonic domain, etc.)

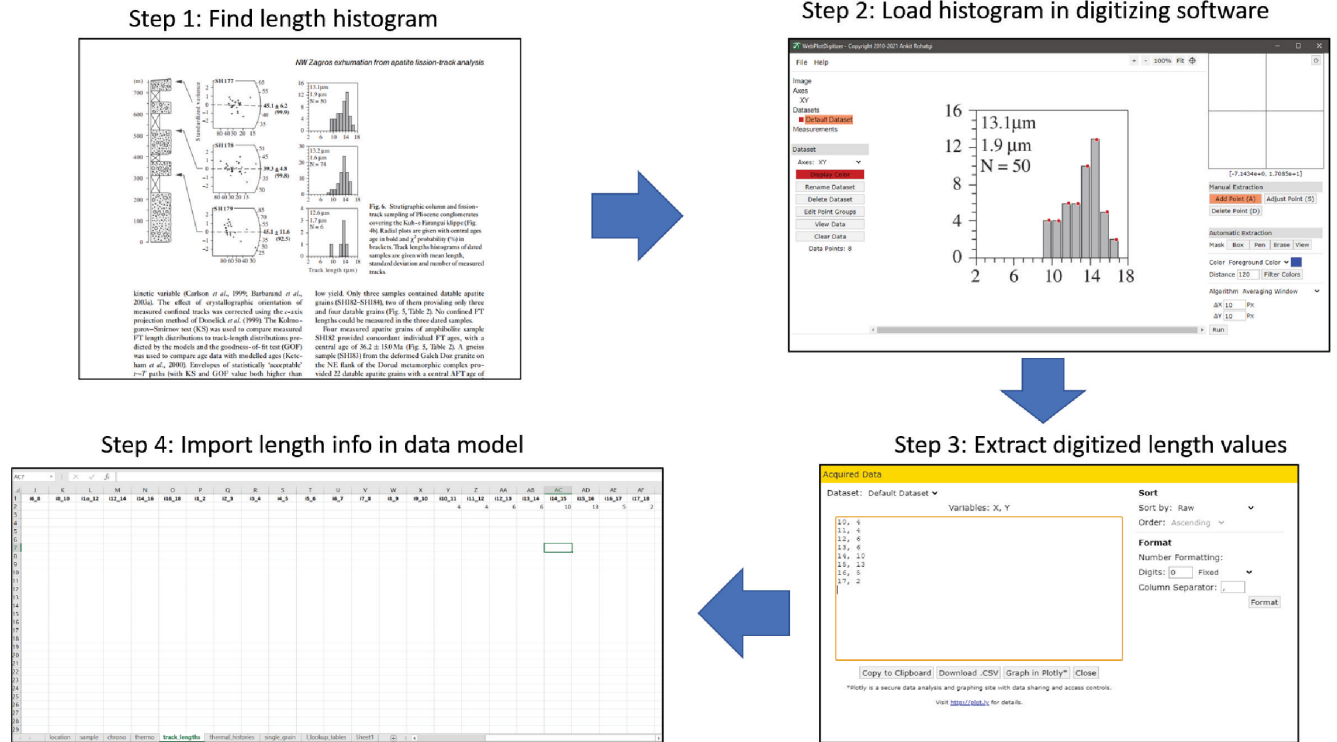


Figure 5. In many older publications the individual measured fission track lengths are only provided as histograms. That information, together with additional information such as kinetic parameters, are essential for modelling thermal histories, so the binned data were digitally extracted from figures in the publications.

Table 1. Glossary of terms for fission track data compilation

FIELD	UNIT	DESCRIPTION	FIELD	UNIT	DESCRIPTION
FT Datapoints			FT Single Grain		
Sample Name		ID of sample analysed	Sample Name		ID of sample analysed
Mineral Name		Mineral type analysed	U (ppm)	ppm	Average U content of analysed grains
FT Age Equation		The equation used to determine FT age	FT Age	Ma	Fission track age
FT U Determination		Analytical method used to measure uranium concentrations for FT age determinations	Age Error (Ma)	Ma	Fission track age uncertainty
Technique			Age Error Type		FT age uncertainty type
Mount ID		ID of analytical batch, allowing related unknown and secondary reference material results to be linked			Mean $rmr0$ of analysed grains, a parameter corresponding to annealing resistance of an apatite grain of certain composition (Carlson et al., 1999; Ketcham et al., 2007)
Number of Grains		Total number of single grains analysed	rmr0		
rhod	cm ⁻²	pd - Mean dosimeter track density	Grain Name		ID of the individual grain dated
nd		Nd - Total number of dosimeter tracks	Population		Distinguishes separate populations within the same sample
rhoS	cm ⁻²	ps - Mean spontaneous track density	Mineral Name		Mineral type analysed
ns		Ns - Total number of spontaneous tracks	FT Length Data		
rhoi	cm ⁻²	pi - Mean induced track density	Etching Time	seconds	Duration of etching
ni		Ni - Total number of induced tracks	Grain Name		Name or lab number of individual grain analysed
U/Ca Ratio		Average U/Ca ratio of analysed grains	Track Type		Type of track measurement (e.g., semi-track, confined track-in-track, confined track-in-cleavages)
U (ppm)	ppm	Average U content of analysed grains	Apparent Length	µm	Apparent length measured parallel to grain surface
U Standard Error (ppm)	ppm	Standard deviation of average U content of analysed grains	Corrected Z Depth	µm	Distance in z-direction between track end points, corrected for retractive index of analysed mineral
chi2pct	%	$P(\chi^2)$ - Chi-square test to statistically test the null-hypothesis that the analysed grains belong to one age population	Azimuth	°C	Azimuth of track
Dispersion		Measure of dispersion of single grain ages, ranging from 0 to 1	Dip	°C	Dip of track
Mean Age (Ma)	Ma	FT mean age	c Axis Angle	°C	Angle of fission track to crystallographic c-axis
Mean Age Error (Ma)	Ma	FT mean age uncertainty	Dpar	µm	Modal etch pit diameter parallel to crystallographic c-axis
Central Age (Ma)	Ma	FT central age	Dper	µm	Modal etch pit diameter perpendicular to crystallographic c-axis
Central Age Error (Ma)	Ma	FT central age uncertainty	rmr0		Parameter corresponding to annealing resistance of an apatite grain of certain composition (Carlson et al., 1999; Ketcham et al., 2007)
Pooled Age (Ma)	Ma	FT pooled age	Comment		Additional information about analysis or data upload
Pooled Age Error (Ma)	Ma	FT pooled age uncertainty	TrackID		Lab number
Age Error Type		FT age uncertainty type	Mineral Name		Mineral type analysed
Population		Distinguishes separate populations within the same sample	FT Binned Length Data		
Population Type		Type of fission track population	Sample Name		Unique name to identify this data entry within the database, useful when uploading associated data (e.g., single grain data)
MTL	µm	Mean confined fission Track Length	DparAvg	µm	Modal etch pit diameter parallel to crystallographic c-axis
MTL 1sc	µm	Standard error of mean confined track length	0x1		Number of measured confined tracks in 0 to 1 micron bin
Number of Tracks		Number of tracks measured	1x2		Number of measured confined tracks in 1 to 2 micron bin
MTL std Dev	µm	Standard deviation of mean confined fission track length	2x3		Number of measured confined tracks in 2 to 3 micron bin
Dpar	µm	Mean etch pit diameter parallel to crystallographic c-axis	3x4		Number of measured confined tracks in 3 to 4 micron bin
DPar Standard Error	µm	Standard error of etch pit diameter parallel to crystallographic c-axis	4x5		Number of measured confined tracks in 4 to 5 micron bin
Dper	µm	Mean etch pit diameter perpendicular to crystallographic c-axis	5x6		Number of measured confined tracks in 5 to 6 micron bin
Dper Standard Error	µm	Standard error of etch pit diameter perpendicular to crystallographic c-axis	6x7		Number of measured confined tracks in 6 to 7 micron bin
rmr0		Mean $rmr0$ of analysed grains, a parameter corresponding to annealing resistance of an apatite grain of certain composition (Carlson et al., 1999; Ketcham et al., 2007)	7x8		Number of measured confined tracks in 7 to 8 micron bin
rmr0 Standard Deviation		Standard deviation of $rmr0$	8x9		Number of measured confined tracks in 8 to 9 micron bin
rmr0 Equation		The equation used to determine the $rmr0$ and κ parameters	9x10		Number of measured confined tracks in 9 to 10 micron bin
Etchant		Etchant chemical composition	10x11		Number of measured confined tracks in 10 to 11 micron bin
Etching Time	seconds	Duration of etching	11x12		Number of measured confined tracks in 11 to 12 micron bin
Etching Temp	°C	Temperature minerals were etched at	12x13		Number of measured confined tracks in 12 to 13 micron bin
Zeta Calibration	yr/cm ²	ζ Calibration - Zeta for EDM or LA-ICP-MS zeta-calibrated fission track ages	13x14		Number of measured confined tracks in 13 to 14 micron bin
Zeta Error	yr/cm ²	Zeta uncertainty for EDM or LA-ICP-MS zeta-calibrated fission track ages	14x15		Number of measured confined tracks in 14 to 15 micron bin
Zeta Error Type		Zeta-calibration uncertainty type	15x16		Number of measured confined tracks in 15 to 16 micron bin
dosimeter		Dosimeter glass used for analysis (only relevant for EDM and population fission track methods)	16x17		Number of measured confined tracks in 16 to 17 micron bin
Irradiation Reactor		Name of irradiation reactor for EDM and population age determinations	17x18		Number of measured confined tracks in 17 to 18 micron bin
Neutron Dose		Thermal neutron dose during sample irradiation (This parameter is only required for fission track ages determined using the Population Method)	18x19		Number of measured confined tracks in 18 to 19 micron bin
Description		Additional information about analysis or data upload	19x20		Number of measured confined tracks in 19 to 29 micron bin
C f Irradiation		Was the sample irradiated with ²⁵² Cf?	Comment		Additional information about analysis or data upload
Reference		ID for any particular publication			
FT Count Data					
Sample Name		ID of sample analysed			
Grain Name		ID of the individual grain dated			
rhoS	cm ⁻²	ps - Spontaneous track density			
ns		Ns - Number of spontaneous tracks			
rhoi	cm ⁻²	pi - Induced track density			
Ni		Number of induced tracks			
Area	cm ²	Total area of counting region			
Dpar	µm	Mean etch pit diameter parallel to crystallographic c-axis			
Population		Distinguishes separate populations within the same sample			
Mineral Name		Mineral type analysed			

Table 2. Glossary of terms for (U-Th)/He data compilation

FIELD	UNIT	DESCRIPTION
FT Datapoints		
Sample Name		ID of sample analysed, usually assigned by sample collector
Mineral		Mineral type analysed
Mean Uncorrected He Age	Ma	Mean uncorrected He age
Mean Corrected He Age	Ma	Mean corrected He age
Mean Corrected He Age	Ma	Mean corrected He age
Uncertainty		Uncertainty of mean corrected He age
Reference		ID for any particular publication
FT Datapoints		
Sample Name		ID of sample analysed, usually assigned by sample collector
AliquotID		Name or lab number of analysed aliquot (if available)
Number of Aliquots		Number of grains in aliquot (only relevant for multi-grain aliquots)
Aliquot Type		The type of aliquot analysed, i.e., single-grain, multi-grain or unknown
Aliquot Length	µm	Length of analysed grain(s) (average value for multi-grain aliquots)
Aliquot Width	µm	Width of analysed grain(s) (average value for multi-grain aliquots)
Aliquot Morphology		Morphology of analysed aliquot grain(s)
Aliquot Mass	mg	Estimated aliquot mass
Aliquot Mass Error	mg	Uncertainty of estimated aliquot mass
4He Amount	ncc	Absolute He content of aliquot
4He Concentration	nmol/g	4He concentration of aliquot
4He Concentration Error	nmol/g	4He concentration uncertainty of aliquot
U Concentration	ppm	Uranium (238U + 235U) concentration of aliquot, calculated as µg/g
U Concentration Error	ppm	Uncertainty of Uranium (238U + 235U) concentration of aliquot, calculated as µg/g
U Concentration Error Type		Uncertainty type
U Amount	ng	Absolute amount of Uranium (238U + 235U) in aliquot
U Amount Error	ng	Uncertainty of absolute amount of Uranium (238U + 235U) in aliquot
U Amount Error Type		Uncertainty type
Th Concentration	ppm	Thorium (232Th) concentration of aliquot, calculated as µg/g
Th Concentration Error	ppm	Uncertainty of Thorium (232Th) concentration of aliquot, calculated as µg/g
Th Concentration Error Type		Uncertainty type
Th Amount	ng	Absolute amount of Thorium (232Th) in aliquot
Th Amount Error	ng	Uncertainty of absolute amount of Thorium (232Th) in aliquot
Th Amount Error Type		Uncertainty type
Sm Concentration	ppm	Samarium (147Sm) concentration of aliquot, calculated as µg/g
Sm Concentration Error	ppm	Uncertainty of Samarium (147Sm) concentration of aliquot, calculated as µg/g
Sm Concentration Error Type		Uncertainty type
eU	ppm	Effective uranium concentration
eU Error	ppm	Effective uranium concentration uncertainty
eU Error Type		Uncertainty type
Th/U		Thorium/Uranium ratio
RSV	µm	Average equivalent spherical radius of analysed aliquot, computed as the radius of a sphere with an equivalent surface area to volume ratio as analysed aliquot
FT		Mass-weighted mean alpha ejection correction (FT) of aliquot
Uncorrected He Age	Ma	Uncorrected He age
Uncorrected He Age Error	Ma	Total analytical uncertainty on uncorrected He age (before FT correction). This should include the propagated uncertainties on the absolute amounts of daughter and parent. See Section 7 in Flowers et al. (2022) for guidance.
Uncorrected He Age Error Type		Uncertainty type
Corrected He Age	Ma	FT corrected He age
Corrected He Age Error	Ma	Total analytical uncertainty on corrected He age (FT corrected). This should include the propagated uncertainties on the absolute amounts of daughter and parent. See Section 7 in Flowers et al. (2022) for guidance.
TAU	Ma	TAU
TAU Error Type		Uncertainty type
Mineral		Mineral type analysed
Comment		Additional information about analysis or data upload

Northern Canada LTT – Compilation and Discussion

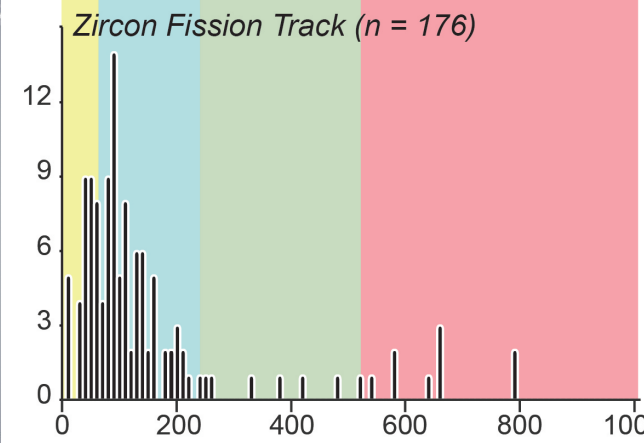
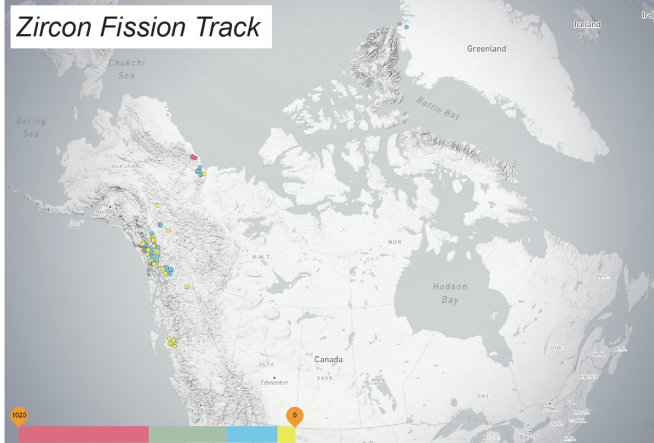
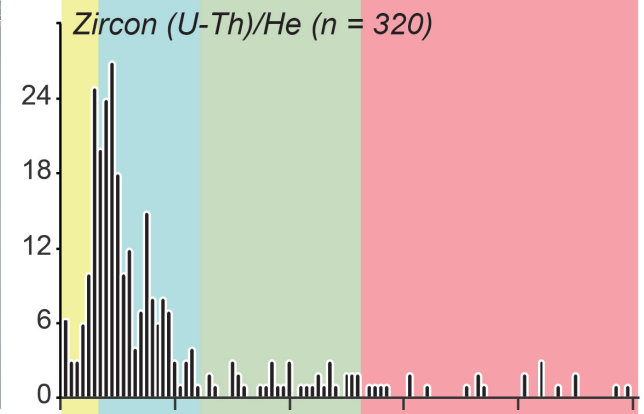
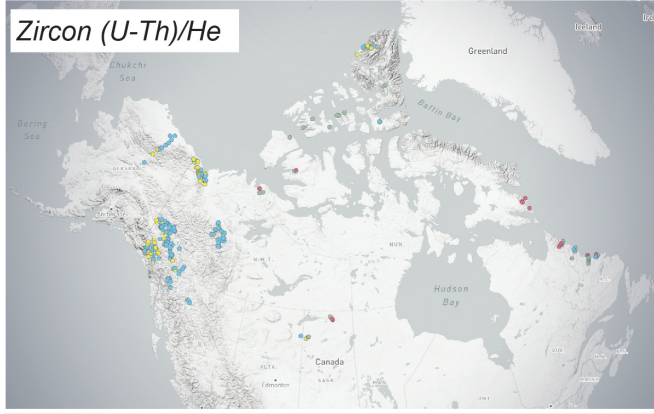
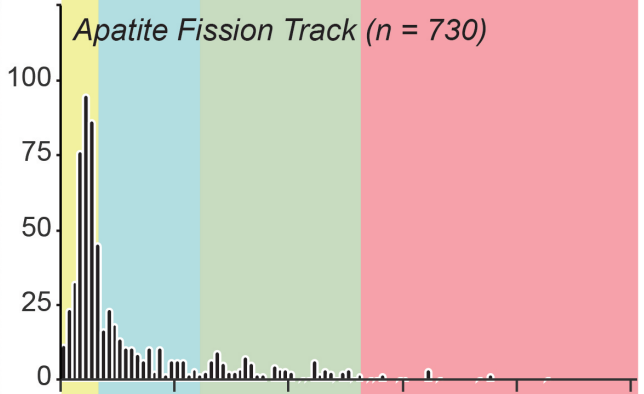
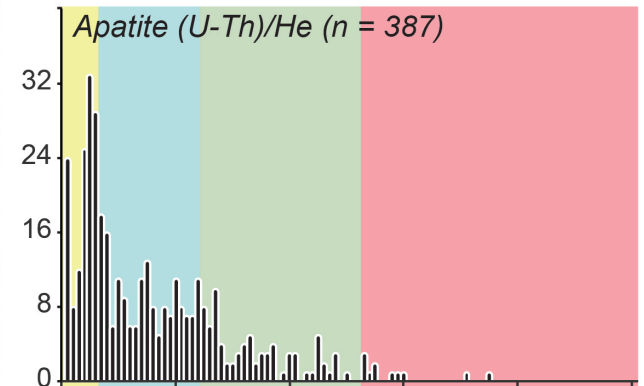
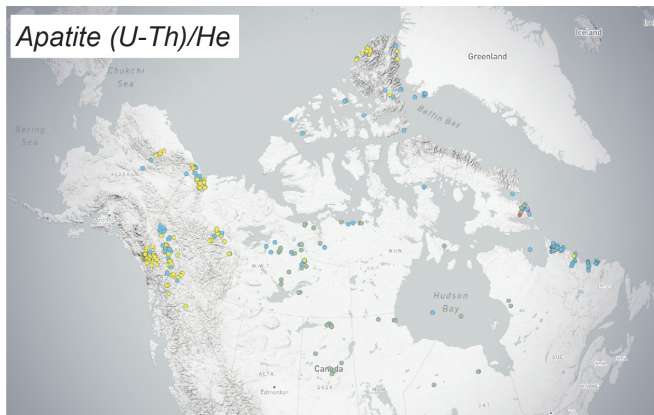
This compilation captures data from 91 different data sources and includes 996 fission track datapoints and 762 (U-Th)/He data points from 1,427 unique samples (Fig. 3). These data are further divided into 16,277 single grain fission track measurements, 27,848 fission track length measurements and 3,230 aliquots of (U-Th)/He data. In Figure 6 the distribution of zircon fission track, zircon (U-Th)/He, apatite fission track and apatite (U-Th)/He data are displayed as a function of age (Precambrian, Paleozoic, Mesozoic, Cenozoic) alongside histograms of the age distributions. In the case of the (U-Th)/He data, where mean ages are not always provided for a sample, Figure 6 displays ages calculated from the single grain ages; while these ages do not properly account for intrasample date-dispersion, they provide a graphical representation of broader trends in the northern Canadian LTT compilation.

The majority of the zircon and apatite (U-Th)/He (ZHe, AHe) and apatite fission track (AFT) data from northern Canada detail cooling related to Mesozoic and younger tectonic systems, such as the Eocene Eureka Orogeny along the northern Arctic margin (e.g. Arne *et al.* 1998, 2002; Vamvaka *et al.* 2019; Powell and Schneider 2022), and the Mesozoic to Eocene northern Canadian Cordillera (e.g. Knight *et al.* 2013; Powell *et al.* 2016, 2020; Bigot-Buschendorf *et al.* 2019; Enkelmann *et al.* 2019; McKay *et al.* 2021; Kellett *et al.* 2023). Compared to the AFT, ZHe and AHe data, there are relatively few zircon fission track (ZFT) dates, many of which represent detrital populations. For example, Precambrian ZFT ages correspond with detrital data from a Neoproterozoic to Cambrian assemblage in the British Mountains of northern Yukon (Bigot-Buschendorf *et al.* 2019) whereas many Cretaceous to Miocene ages are from glacial-fluvial drainage studies along the border between British Columbia, Yukon and Alaska (Enkelmann and Falkowski 2021). The few ZFT data from bedrock samples are also located in southwestern Yukon and northwestern British Columbia and detail cooling related to Mesozoic terrane accretion (e.g. Enkelmann *et al.* 2017).

If LTT are abundant for the younger orogens, there is a notable paucity of data from other geologically important regions. For example, the relative absence of LTT data in the Arctic Islands results in poor quantitative constraints on the timing and magnitude of: 1) burial and exhumation in the Franklinian Basin and Sverdrup Basin; and 2) circum-Arctic tectonic events such as rifting and seafloor spreading associated with the opening of the Arctic Ocean. Similarly, LTT data are mostly absent across the Canadian Shield. The few existing studies (e.g. Willett *et al.* 1997; Issler *et al.* 1999; Flowers *et al.* 2006a, 2009; Kohlmann 2010, Ault *et al.* 2013) suggest that the ‘stable’ cratonic interior is fairly dynamic through deep geologic time, subsiding and unroofing in response to far-field stresses.

Another insight from Figure 6 is that few studies present multiple thermochronometers for each sample. This is potentially due to the fact that LTT data acquisition is time consuming and expensive, and that few laboratories are equipped for both fission track and (U-Th)/He analysis. Moreover, many studies have shown that the temperature sensitivity of the LTT methods can overlap depending on mineral composition and thermal history (Guenther *et al.* 2013; McDannell *et al.* 2019; Powell *et al.* 2020; Issler *et al.* 2022) causing some researchers to consider complimentary thermochronometers redundant. However, the absence of multi-chronometer samples may also result in studies that provide an incomplete record of upper crustal thermal histories, or statistical leveling issues between datasets. Studies that combine ZFT, ZHe, AFT and AHe would be particularly useful in the Canadian Shield as cratonic rocks provide a natural laboratory to test how well experimental studies of diffusion and annealing are extrapolated through deep time.

Figure 6. (next page) Illustrating the distribution of LTT data, and their corresponding ages, for the northern Canada LTT compilation. Thermochronometers are plotted in order of increasing temperature sensitivity. Samples on the map are coloured corresponding to their age (red = Precambrian, green = Paleozoic, blue = Mesozoic, yellow = Cenozoic)



Age (Myr)

Conclusions

This open file details a comprehensive compilation of low temperature thermochronology data from northern Canada. This compilation is the first step towards the Geological Survey of Canada's Canadian ThermoCHronology (CATCH) database. Subsequent publications will detail a compilation of data from southern Canada, thermal histories for all Canadian samples, and templates for uploading data from future publications to the CATCH database.

Acknowledgements

This project was funded through the GeoMapping for Energy and Minerals (GEM) GeoNorth project. We thank Nicolas Pinet, Dale Issler, Lisel Currie, David Schneider, Eva Enkelmann, Isabelle Coutand, Marcos Zentilli, Becky Flowers, and Alexis Ault for their assistance in locating publications, unpublished datasets and for providing their thoughts on the pertinent fields for the data compilation. This report benefited from the helpful review of Lisel Currie.

References

- Armstrong, P.A. 2005. Thermochronometers in sedimentary basins. *Reviews in Mineralogy and Geochemistry*, **58**, 499–525, <https://doi.org/10.2138/rmg.2005.58.19>.
- Arne, D.C., Zentilli, M., Grist, A.M. and Collins, M. 1998. Constraints on the timing of thrusting during the Eureka orogeny, Canadian arctic archipelago: An integrated approach to thermal history analysis. *Canadian Journal of Earth Sciences*, **35**, 30–38, <https://doi.org/10.1139/cjes-35-1-30>.
- Arne, D.C., Grist, A.M., Zentilli, M., Collins, M., Embry, A. and Gentzis, T. 2002. Cooling of the Sverdrup Basin during Tertiary basin inversion: Implications for hydrocarbon exploration. *Basin Research*, **14**, 183–205, <https://doi.org/10.1046/j.1365-2117.2002.00163.x>.
- Ault, A.K., Flowers, R.M. and Bowring, S.A. 2013. Phanerozoic surface history of the Slave craton. *Tectonics*, **32**, 1066–1083, <https://doi.org/10.1002/tect.20069>.
- Bigot-Buschendorf, M., Mouthereau, F., Labrousse, L., Fillon, C., Stübner, K. and Bernet, M. 2019. Unravelling the thermal evolution of the Neruokpuk Formation in the British Mountains, North Yukon, Canada: Tectonic and orogenic implications. In: *Circum-Arctic Structural Events: Tectonic Evolution of the Arctic Margins and Trans-Arctic Links with Adjacent Orogens*. 619–635., [https://doi.org/10.1130/2018.2541\(26\)](https://doi.org/10.1130/2018.2541(26)).
- Boone, S.C., Kohlmann, F., et al. 2023. A geospatial platform for the tectonic interpretation of low-temperature thermochronology Big Data. *Scientific Reports*, **13**, 1–15, <https://doi.org/10.1038/s41598-023-35776-3>.
- Carlson, W.D., Donelick, R.A. and Ketchum, R.A. 1999. Variability of apatite fission-track annealing kinetics: I. Experimental results. *American Mineralogist*, **84**, 1213–1223, <https://doi.org/10.2138/am-1999-0902>.
- Djimbi, D.M., Gautheron, C., Roques, J., Tassan-Got, L., Gerin, C. and Simoni, E. 2015. Impact of apatite chemical composition on (U-Th)/He thermochronometry: An atomistic point of view. *Geochimica et Cosmochimica Acta*, **167**, 162–176, <https://doi.org/10.1016/j.gca.2015.06.017>.
- Enkelmann, E. and Falkowski, S. 2021. Deformation between the highly oblique Yakutat–North American plate boundary and the Eastern Denali fault. *Geosphere*, **17**, 2123–2143, <https://doi.org/10.1130/GES02410.1>.
- Enkelmann, E., Piestrzeniewicz, A., Falkowski, S., Stübner, K. and Ehlers, T.A. 2017. Thermochronology in southeast Alaska and southwest Yukon: Implications for North American Plate response to terrane accretion. *Earth and Planetary Science Letters*, **457**, 348–358,

- <https://doi.org/10.1016/j.epsl.2016.10.032>.
- Enkelmann, E., Finzel, E. and Arkle, J. 2019. Deformation at the eastern margin of the Northern Canadian Cordillera: Potentially related to opening of the North Atlantic. *Terra Nova*, **31**, 151–158, <https://doi.org/10.1111/ter.12374>.
- Farley, K.A., Wolf, R.A. and Silver, L.T. 1996. The effects of long alpha-stopping distances on (U-Th)/He ages. *Geochimica et Cosmochimica Acta*, **60**, 4223–4229, [https://doi.org/10.1016/S0016-7037\(96\)00193-7](https://doi.org/10.1016/S0016-7037(96)00193-7).
- Flowers, R.M. 2009. Exploiting radiation damage control on apatite (U-Th)/He dates in cratonic regions. *Earth and Planetary Science Letters*, **277**, 148–155, <https://doi.org/10.1016/j.epsl.2008.10.005>.
- Flowers, R.M., Bowring, S.A. and Reiners, P.W. 2006. Low long-term erosion rates and extreme continental stability documented by ancient (U-Th)/He dates. *Geology*, **34**, 925–928, <https://doi.org/10.1130/G22670A.1>.
- Flowers, R.M., Ketcham, R.A., Shuster, D.L. and Farley, K.A. 2009. Apatite (U-Th)/He thermochronometry using a radiation damage accumulation and annealing model. *Geochimica et Cosmochimica Acta*, **73**, 2347–2365, <https://doi.org/10.1016/j.gca.2009.01.015>.
- Flowers, R.M., Zeitler, P.K., et al. 2023a. (U-Th)/He chronology: Part 1. Data, uncertainty, and reporting. *GSA Bulletin*, **135**, 104–136, <https://doi.org/10.1130/B36266.1>.
- Flowers, R.M., Ketcham, R.A., et al. 2023b. (U-Th)/He chronology: Part 2. Considerations for evaluating, integrating, and interpreting conventional individual aliquot data. *GSA Bulletin*, **135**, 137–161, <https://doi.org/10.1130/B36268.1>.
- Fox, M., Herman, F., Willett, S.D. and May, D.A. 2014. A linear inversion method to infer exhumation rates in space and time from thermochronometric data. *Earth Surface Dynamics*, **2**, 47–65, <https://doi.org/10.5194/esurf-2-47-2014>.
- Fox, M., Herman, F., Willett, S.D. and Schmid, S.M. 2016. The exhumation history of the European alps inferred from linear inversion of thermochronometric data. *American Journal of Science*, **316**, 505–541, <https://doi.org/10.2475/06.2016.01>.
- Gallagher, K. 2012. Transdimensional inverse thermal history modeling for quantitative thermochronology. *Journal of Geophysical Research: Solid Earth*, **117**, <https://doi.org/10.1029/2011JB008825>.
- Gallagher, K. 2023. Trans-Dimensional Markov Chain Monte Carlo Methods Applied to Geochronology and Thermochronology. In: *Applications of Data Assimilation and Inverse Problems in the Earth Sciences*. 175–195., <https://doi.org/10.1017/9781009180412.012>.
- Gautheron, C., Tassan-Got, L., Barbarand, J. and Pagel, M. 2009. Effect of alpha-damage annealing on apatite (U-Th)/He thermochronology. *Chemical Geology*, **266**, 157–170, <https://doi.org/10.1016/j.chemgeo.2009.06.001>.
- Gleadow, A.J.W. and Duddy, I.R. 1981. A natural long-term track annealing experiment for apatite. *Nuclear Tracks*, **5**, 169–174, [https://doi.org/10.1016/0191-278X\(81\)90039-1](https://doi.org/10.1016/0191-278X(81)90039-1).
- Green, P.F. 1980. On the cause of the shortening of spontaneous fission tracks in certain minerals. *Nuclear Tracks*, **4**, 91–100, [https://doi.org/10.1016/0191-278X\(80\)90018-9](https://doi.org/10.1016/0191-278X(80)90018-9).
- Guenther, W.R., Reiners, P.W., Ketcham, R.A., Nasdala, L. and Giester, G. 2013. Helium diffusion in natural zircon: radiation damage, anisotropy, and the interpretation of zircon (U-TH)/He thermochronology. *American Journal of Science*, **313**, 145–198, <https://doi.org/10.2475/03.2013.01>.
- Issler, D.R. 1996. An inverse model for extracting thermal histories from apatite fission track data: instructions and software for the Windows 95 environment. *Geological Survey of Canada, Open File 2325*, 84, <https://doi.org/10.4095/208313>.
- Issler, D.R., Beaumont, C., Willett, S.D., Donelick, R.A. and Grist, A.M. 1999. Paleotemperature history of two transects across the Western Canada Sedimentary Basin: Constraints from apatite

- fission track analysis. *Bulletin of Canadian Petroleum Geology*, **47**, 475–486.
- Issler, D.R., McDannell, K.T., O’Sullivan, P.B. and Lane, L.S. 2022. Simulating sedimentary burial cycles – Part 2: Elemental-based multikinetic apatite fission-track interpretation and modelling techniques illustrated using examples from northern Yukon. *Geochronology*, **4**, 373–397, <https://doi.org/10.5194/gchron-4-373-2022>.
- Kellett, D.A., Coutand, I., Zagorevski, A., Grujic, D., Dewing, K. and Beranek, L. 2023. Whitehorse Trough records Late Triassic–Cretaceous accretionary orogenesis in the Northern Canadian Cordillera via detrital mineral thermochronometry. *Canadian Journal of Earth Sciences*, **61**, 223–247, <https://doi.org/10.1139/cjes-2023-0082>.
- Ketcham, R.A. 2005. Forward and Inverse Modeling of Low-Temperature Thermochronometry Data. *Reviews in Mineralogy and Geochemistry*, **58**, 275–314, <https://doi.org/10.2138/rmg.2005.58.11>.
- Ketcham, R.A. 2024. Thermal history inversion from thermochronometric data and complementary information: New methods and recommended practices. *Chemical Geology*, 122042, <https://doi.org/10.1016/j.chemgeo.2024.122042>.
- Ketcham, R.A., Donelick, R.A. and Carlson, W.D. 1999. Variability of apatite fission-track annealing kinetics: III. Extrapolation to geological time scales. *American Mineralogist*, **84**, 1235–1255, <https://doi.org/10.2138/am-1999-0902>.
- Knight, E., Schneider, D.A. and Ryan, J. 2013. Thermochronology of the Yukon-Tanana Terrane, West-Central Yukon: Evidence for Jurassic Extension and Exhumation in the Northern Canadian Cordillera. *The Journal of Geology*, **121**, 371–400, <https://doi.org/10.1086/670721>.
- Kohlmann, F. 2010. Insights into the nanoscale formation of fission tracks in solids and a low temperature thermochronology study of the Archean Slave Province, Northwest Territories, Canada. PhD Thesis, The University of Melbourne, 303pp.
- Kohn, B.P., Ketcham, R.A., et al. 2024. Interpreting and reporting fission-track chronological data. *Geological Society of America Bulletin*, <https://doi.org/10.1130/B37245.1>.
- McDannell, K.T., Issler, D.R. and O’Sullivan, P.B. 2019. Radiation-enhanced fission track annealing revisited and consequences for apatite thermochronometry. *Geochimica et Cosmochimica Acta*, **252**, 213–239, <https://doi.org/10.1016/j.gca.2019.03.006>.
- McKay, R., Enkelmann, E., Hadlari, T., Matthews, W. and Mouthereau, F. 2021. Cenozoic Exhumation History of the Eastern Margin of the Northern Canadian Cordillera. *Tectonics*, **40**, <https://doi.org/10.1029/2020TC006582>.
- Naeser, C.W. 1967. The use of apatite and sphene for fission track determinations. *GSA Bulletin*, **78**, 1523–1526, [https://doi.org/10.1130/0016-7606\(1967\)78\(1523:TUOAAAS\)2.0.CO](https://doi.org/10.1130/0016-7606(1967)78(1523:TUOAAAS)2.0.CO).
- Pinet, N., & Brake, V. (2018). Preliminary compilation of apatite fission-track data in Canada. *Geological Survey of Canada, Open File 8454*. <https://doi.org/10.4095/308443>
- Powell, J., Schneider, D., Stockli, D. and Fallas, K. 2016. Zircon (U-Th)/He thermochronology of Neoproterozoic strata from the Mackenzie Mountains, Canada: Implications for the Phanerozoic exhumation and deformation history of the northern Canadian Cordillera. *Tectonics*, **35**, 663–689, <https://doi.org/10.1002/2015TC003989>.
- Powell, J.W. and Schneider, D.A. 2022. Phanerozoic Record of Northern Ellesmere Island, Canadian High Arctic, Resolved Through $40\text{ Ar}/39\text{ Ar}$ and (U-Th)/He Geochronology. *Tectonics*, **41**, <https://doi.org/10.1029/2021TC007065>.
- Powell, J.W., Issler, D.R., Schneider, D.A., Fallas, K.M. and Stockli, D.F. 2020. Thermal history of the Mackenzie Plain, Northwest Territories, Canada: Insights from low-temperature thermochronology of the Devonian Imperial Formation. *GSA Bulletin*, **132**, 767–783, <https://doi.org/10.1130/B35089.1>.
- Price, P.B. and Walker, R.M. 1963. Fossil tracks of charged particles in mica and the age of minerals. *Journal of Geophysical Research*, **68**, 4847–4862, <https://doi.org/10.1029/JZ068i016p04847>.
- Reiners, P.W. and Brandon, M.T. 2006. Using Thermochronology To Understand Orogenic Erosion.

- Annual Review of Earth and Planetary Sciences*, **34**, 419–466, <https://doi.org/10.1146/annurev.earth.34.031405.125202>.
- Shuster, D.L., Flowers, R.M. and Farley, K.A. 2006. The influence of natural radiation damage on helium diffusion kinetics in apatite. *Earth and Planetary Science Letters*, **249**, 148–161, <https://doi.org/10.1016/j.epsl.2006.07.028>.
- Strutt, R.J. 1909. The accumulation of helium in geological time.-II. *Proceedings of the Royal Society of London. Series A, Containing Papers of a Mathematical and Physical Character*, **83**, 96–99, <https://doi.org/10.1098/rspa.1909.0081>.
- Strutt, R.J. 1910. The accumulation of helium in geological time.—III. *Proceedings of the Royal Society of London. Series A, Containing Papers of a Mathematical and Physical Character*, **83**, 298–301, <https://doi.org/10.1098/rspa.1910.0017>.
- Vamvaka, A., Pross, J., Monien, P., Piepjohn, K., Estrada, S., Lisker, F. and Spiegel, C. 2019. Exhuming the Top End of North America: Episodic Evolution of the Eureka Belt and Its Potential Relationships to North Atlantic Plate Tectonics and Arctic Climate Change. *Tectonics*, **38**, 4207–4228, <https://doi.org/10.1029/2019TC005621>.
- van der Beek, P. and Schildgen, T.F. 2023. Short communication: age2exhume – a MATLAB/Python script to calculate steady-state vertical exhumation rates from thermochronometric ages and application to the Himalaya. *Geochronology*, **5**, 35–49, <https://doi.org/10.5194/gchron-5-35-2023>.
- Wagner, G.A. 1968. Fission track dating of apatites. *Earth and Planetary Science Letters*, **4**, 411–415, [https://doi.org/10.1016/0012-821X\(68\)90072-1](https://doi.org/10.1016/0012-821X(68)90072-1).
- Willett, S.D., Issler, D.R., Beaumont, C., Donelick, R.A. and Grist, A.M. 1997. Inverse modeling of annealing of fission tracks in apatite 2: Application to the thermal history of the Peace River Arch region, Western Canada sedimentary basin. *American Journal of Science*, **297**, 970–1011, <https://doi.org/10.2475/ajs.297.10.970>.
- Zeitler, P.K., Herczeg, A.L., McDougall, I. and Honda, M. 1987. U-Th-He dating of apatite: A potential thermochronometer. *Geochimica et Cosmochimica Acta*, **51**, 2865–2868, [https://doi.org/10.1016/0016-7037\(87\)90164-5](https://doi.org/10.1016/0016-7037(87)90164-5).